

# Study of the Diurnal Cycle of Microphysical Properties of Clouds in the Amazon Basin Using GOES Measurements

Pugliesi Silva, A. C.<sup>1</sup>, Correia, A. L.<sup>1</sup>, and Monteiro, M. M.<sup>1</sup>  
<sup>1</sup>Institute of Physics, University of São Paulo, São Paulo, Brazil  
 Email correspondence: [andre.cezar.silva@gmail.com](mailto:andre.cezar.silva@gmail.com)



## Methodology, Data acquisition and Objectives



Figure 1: Selected area.

The Amazon Basin plays a key role in Earth's hydrological cycle and in the planetary energy budget. One key aspect is understanding the influence of aerosols on cloud microphysics, cloud formation and evolution [1].

In this work, we used a set of radiance measurements from channels 1, 2 and 4 (0.63, 3.9 and 11  $\mu\text{m}$ , respectively) of NOAA's Geostationary Operational Satellite (GOES-13) [2]. These images were obtained on the largest yellow square shown in the map (2°N, 70°W, 49°W, 16°S) (Fig. 1) between 2010 and 2014.

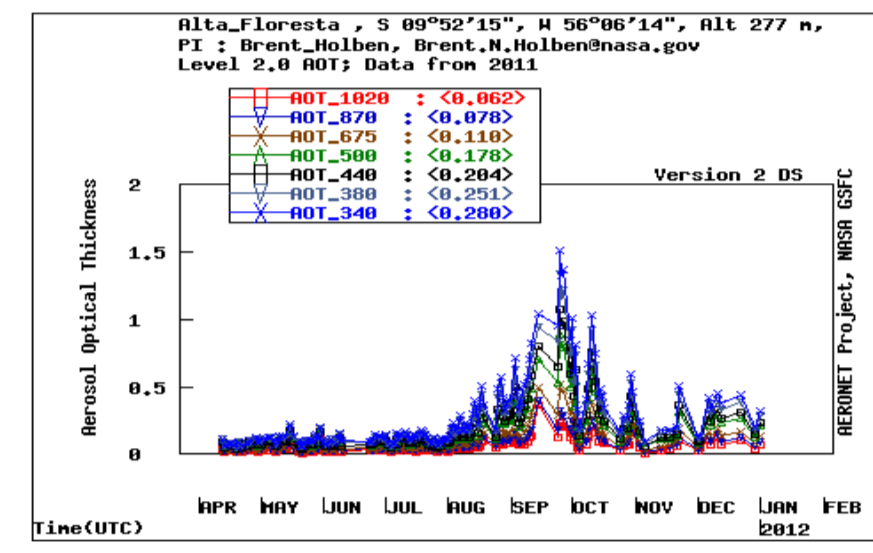


Figure 2: Monthly Aerosol Optical Thickness during 2011.

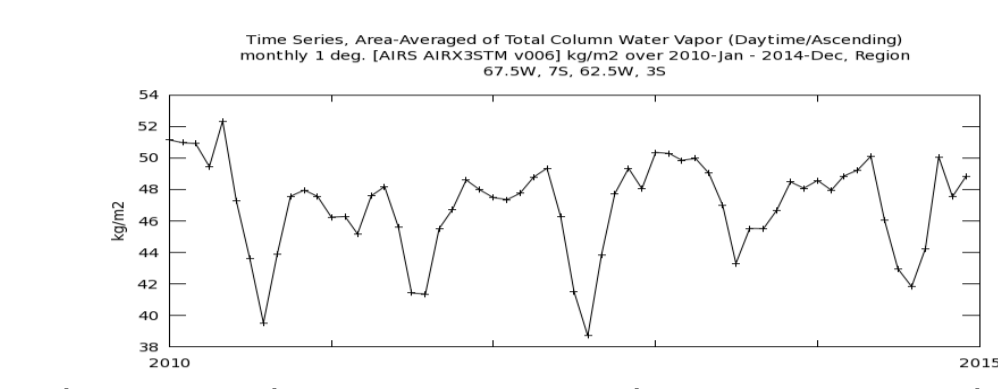


Figure 3: Column Water Vapor between 2010 and 2015.

The analyzed data are in a ~40000 km<sup>2</sup> pristine forest region (small yellow square), divided in three seasons: humid, dry (without pollution), and biomass burning. These seasons were defined using data from AERONET [3] (Fig. 2) and NASA's Giovanni website [4] (Fig. 3). The libRadtran radiative transfer code [5] was used to obtain estimates of the effective radius of droplets and ice particles in convective clouds.

## Visible, Near and Thermal Infrared Channels

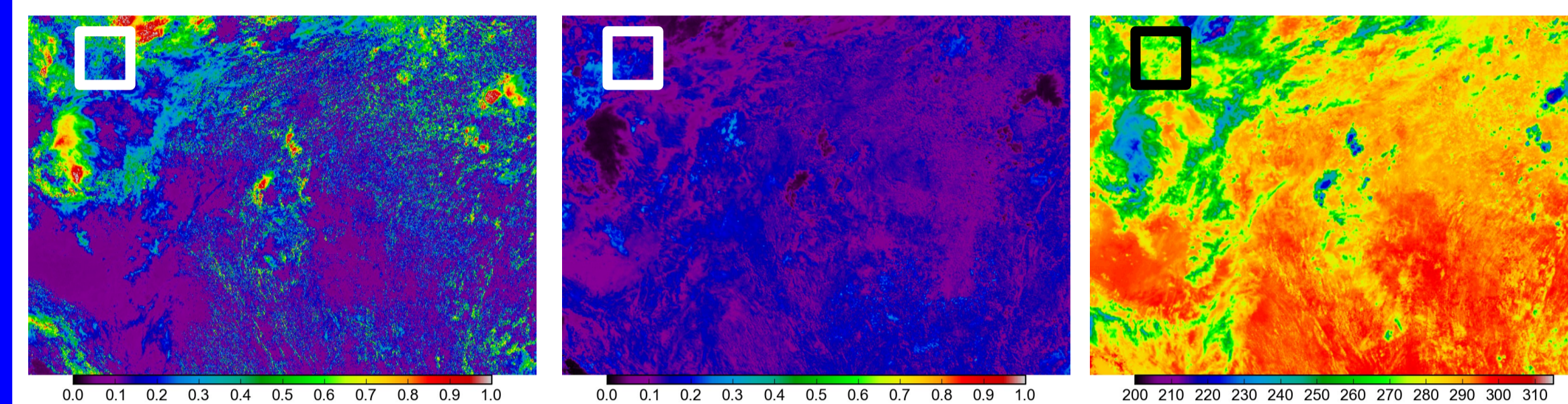


Figure 4: Reflectance on channel 1. April 08, 2014 (wet season) at 10:45 LT

Figure 5: Reflectance on channel 2.

Figure 6: Brightness Temperature on channel 4.

Figures 4, 5 and 6 show examples of reflectance results on 0.63  $\mu\text{m}$ , 3.90  $\mu\text{m}$ , and brightness temperature on 11  $\mu\text{m}$ , respectively. The highlighted squares show the region where the analyses were performed. The images were obtained by a Python script that takes into account the GOES 13 satellite calibration constants [6], and geometrical conditions of solar zenith angle and the satellite's view zenith angle. From these images it is possible to analyze cloud top temperatures, cloud cover, and infer cloud droplet/ice particle size, under different meteorological conditions and availability of aerosols.

## Temperature by Effective Radius 2D Histograms for different seasons

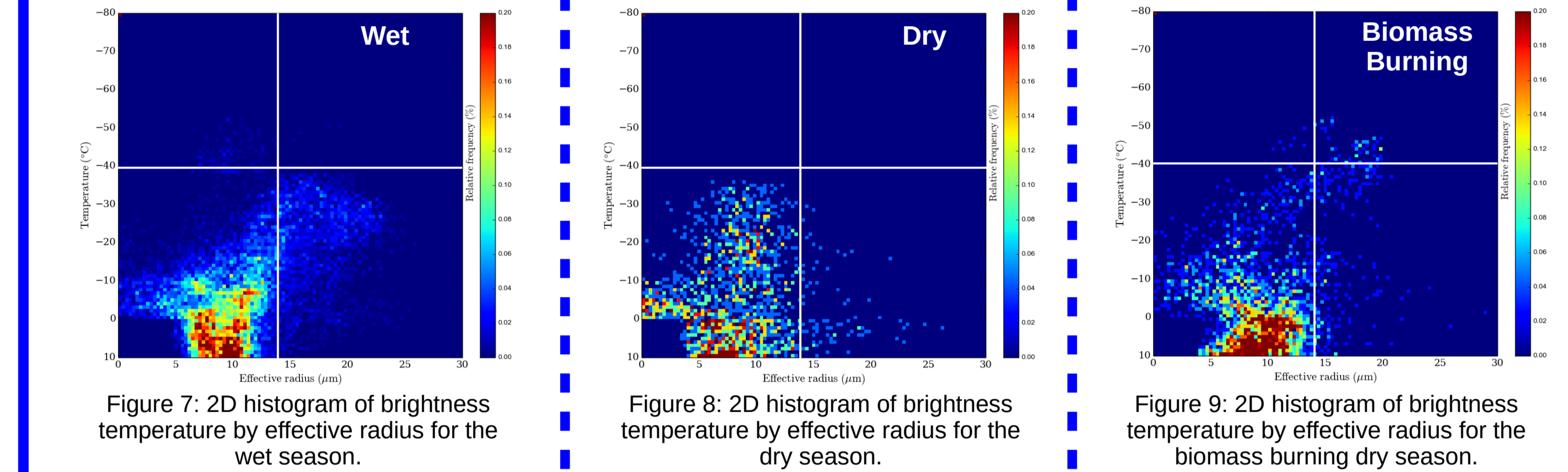


Figure 7: 2D histogram of brightness temperature by effective radius for the wet season.

Figure 8: 2D histogram of brightness temperature by effective radius for the dry season.

Figure 9: 2D histogram of brightness temperature by effective radius for the biomass burning dry season.

Figures 7, 8 and 9 show 2D histograms of seasonal averages of brightness temperature as a function of the effective radius for cloud pixels, between 2010 and 2014. The wet season displays a relatively denser distribution of low clouds and less frequent tops colder than -40°C, with mixed phase droplet size growth. The dry season shows relatively more scatter and less evident mixed phase droplet growth. The biomass burning season shows in average a strong density of warmer clouds, but also the occurrence of very cold cloud tops.

## Temperature by Effective Radius for Cloud Pixels on different seasons over the Amazon Basin

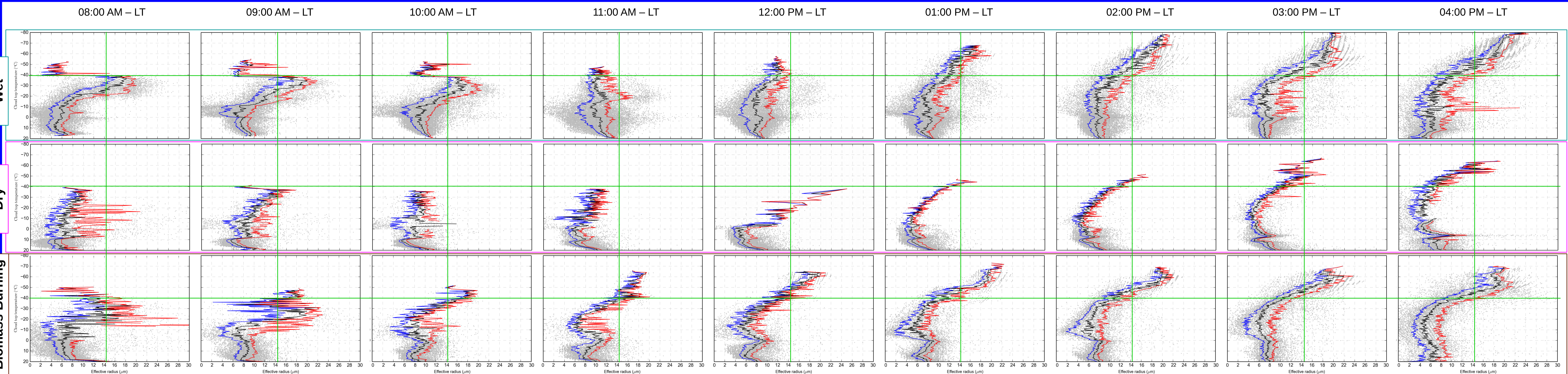


Figure 10: Diurnal cycle of microphysical properties of Clouds over the Amazon basin in wet, dry and burning biomass dry seasons.

Figure 10 shows the diurnal evolution of temperature values as a function of effective radius for cloud pixels. The top line corresponds to 5-year hourly averages of a representative day in the wet season. The middle and bottom lines correspond to the dry and biomass burning seasons, respectively. The blue, black, and red lines represent the 25<sup>th</sup>, 50<sup>th</sup>, and 75<sup>th</sup> percentiles, respectively. In the wet season, which has more data points, in average clouds start forming with relatively smaller droplets and warmer tops early in the morning; by noon droplets are bigger and deep convection starts to develop, with cloud tops reaching temperatures below -40°C. Regarding the dry season, less clouds are formed, as evidenced by the smaller number of data points. In spite of this, it is possible to see that the clouds in the dry season are warmer than in the wet season, in average. Throughout the day the values of effective radius increase, but not as strongly as in the wet season. During the biomass burning season, with higher aerosol availability in the atmosphere, mixed phase clouds (temperatures between 0°C and -40°C) reach lower temperatures in average (and with larger effective radii) along the day. This occurs faster than in the dry season without pollution. For low and warm clouds (with temperatures above 0°C), the droplet effective radius decreases over time. Comparing the graphs at 1:00PM LT, it is evident that the wet and biomass burning seasons have more cloud pixels with lower temperatures and high effective radii than the dry season. However, this occurs much more rapidly in the biomass burning season, that shows a relatively fast behavior in increasing the values of the effective radius. This can occur due to the greater presence of aerosols in the atmosphere.

## References

- [1] - Poschl, U., Martin, S., Sinha, B., Chen, Q., Gunthe, S. et al.: Rainforest Aerosols as Biogenic Nuclei of Clouds and Precipitation in the Amazon, Science, 329, 1513-1516, doi:10.1126/science.1191056, 2010.
- [2] - <https://www.class.ncdc.noaa.gov/saa/products/welcome>
- [3] - [https://aeronet.gsfc.nasa.gov/cgi-bin/type\\_one\\_station\\_opera\\_v2\\_new?site=Alta\\_Floresta&nachal=0&year=20&aero\\_water=0&level=3&if\\_day=0&if\\_err=0&place\\_code=10&year\\_or\\_month=1](https://aeronet.gsfc.nasa.gov/cgi-bin/type_one_station_opera_v2_new?site=Alta_Floresta&nachal=0&year=20&aero_water=0&level=3&if_day=0&if_err=0&place_code=10&year_or_month=1)
- [4] - [https://giovanni.sci.gsfc.nasa.gov/giovanni/#service=ArAVTs&starttime=2010-01-01T00:00:00Z&endtime=2014-12-31T23:59:59Z&bbox=-67.5,-7,-62.5,-3&data=AIRX3STM\\_006\\_TotH2OVap\\_A](https://giovanni.sci.gsfc.nasa.gov/giovanni/#service=ArAVTs&starttime=2010-01-01T00:00:00Z&endtime=2014-12-31T23:59:59Z&bbox=-67.5,-7,-62.5,-3&data=AIRX3STM_006_TotH2OVap_A)
- [5] - Emde, C., Buras-Schnell, R., Kylling, A., Mayer, B., Gasteiger, J., Hamann et al.: The libRadtran software package for radiative transfer calculations (version 2.0.1), Geosci. Model Dev., 9, 1647-1672, doi:10.5194/gmd-9-1647-2016, 2016.
- [6] - <http://www.ospo.noaa.gov/Operations/GOES/calibration/gvar-conversion.html>

## Acknowledgements

This research is funded by the Coordination of Higher Education (CAPES), a foundation linked to the Brazilian Ministry of Education (MEC), to which we are grateful. A. Correia thanks FAPESP grant 2010/15959-3.